

# Evidence of Scaling Regimes in the Hopfield Dynamics of Whole Brain Model

Giorgio Gosti,<sup>1,2</sup> Sauro Succi,<sup>1,3</sup> and Giancarlo Ruocco<sup>1,4</sup>

<sup>1</sup>*Center for Life Nano- and Neuro-Science, Istituto Italiano di Tecnologia,  
Viale Regina Elena 201, I-00161, Rome, Italy*

<sup>2</sup>*Istituto di Scienze del Patrimonio Culturale, Sede di Roma,  
Consiglio Nazionale delle Ricerche, 00010, Montelibretti (RM), Italy*

<sup>3</sup>*Istituto per le Applicazioni del Calcolo del Consiglio Nazionale  
delle Ricerche, via dei Taurini 19, I-00185, Rome, Italy*

<sup>4</sup>*Dipartimento di Fisica, Università di Roma “La Sapienza”, P.le Aldo Moro 5, I-00185, Roma, Italy*

(Dated: January 17, 2024)

It is shown that a Hopfield recurrent neural network, informed by experimentally derived brain topology, recovers the scaling picture recently introduced by Deco [1], according to which the process of information transfer within the human brain shows spatially correlated patterns qualitatively similar to those displayed by turbulent flows. Although both models employ a coupling strength which decays exponentially with the euclidean distance between the nodes, their mathematical nature is widely different, Hopf oscillators versus Hopfield neural network. Hence, their convergence suggests a remarkable robustness of the aforementioned scaling picture. Furthermore, the present analysis shows that the Hopfield model brain remains functional by removing links above about five decay lengths, corresponding to about one sixth of the size of the global brain. This suggests that, in terms of connectivity decay length, the Hopfield brain functions in a sort of intermediate “turbulent liquid”-like state, whose essential connections are the intermediate ones between the connectivity decay length and the global brain size. This “turbulent-like liquid” appears to be more spiky than actual turbulent fluids, with a scaling exponent around 2/5 instead of 2/3.

## INTRODUCTION

In a recent paper [1], it was argued that the information transfer within the human brain may proceed in close analogy with the mechanisms which govern mass and energy transport in turbulent fluids. The analogy refers to the emergence of correlated spacetime patterns which would facilitate and possibly optimize information transfer across the brain, the “same” way as fluid turbulence enhances energy transport across fluids. Based on an extended dynamical system of oscillators (Hopf model), supplemented by large-scale neuro-imaging empirical data on the connections between different brain areas, the authors of [1] numerically showed that the statistical correlations of human brain signals may exhibit a scaling regime similar to the one observed in turbulent fluids.

At a closer scrutiny, though, the analogy does not appear to be quantitative, meaning that the spatial scaling exponents of the second order structure function  $S_2(d) = \langle (O(d) - O(0))^2 \rangle \sim d^\alpha$ ,  $O$  being a suitable order parameter, are not the same, about  $\alpha \sim 1/2$  for the Hopf model of the human brain against  $\alpha=2/3$  for fluid turbulence. Yet, a scaling regime in space is found in either cases, which is intriguing *per se*, regardless of the specific value of  $\alpha$ .

In this paper, we probe the robustness of the above analogy by performing a similar analysis based

on the same neuro-data, but using a very different model, namely a Hopfield neural network, and measuring scaling exponents as a function of the connectivity decay length  $\delta$ .

The recurrent Hopfield neural network model is a well-established model for small-scale neuronal networks [2–4]. It is a neural network model based on binary McCulloch-Pitts neurons [5–8] in which every processing unit ( $i$ ) is connected to all the other ones ( $j$ ) through a set of weights ( $J_{ij}$ ). Most of the literature considers fully connected and symmetric Hopfield networks since this simplifies the mathematical analysis of the model, although recently the investigation of diluted networks [6, 9–12] and asymmetric networks [11–18] was introduced.

Usually, a recurrent Hopfield neural network is trained to store patterns or memories as steady state attractors with the Hebbian prescription. In this case, the coupling matrix  $J_{ij}$  assumes the form of the sum of diadic forms, it is therefore symmetric and fully connected. The maximum storage capacity of such a network is found to be linear with the number of nodes  $N$ . The capacity can be increased by the process of learning (Hebbian learning): in this process the simultaneous activation of two nodes will strengthen their connection. This is inspired by biological neural networks where the simultaneous activation of neurons leads to increments in synaptic strength [20], and it allows the network to store a larger number of patterns [5], but this quantity still

remains linear with  $N$ . Lately, researchers have also investigated how unlearning methods can improve the stability of the stored patterns [21–23].

Interestingly, it has been recently demonstrated both numerically [11, 24] and theoretically [25, 26] that *random*, non-Hebbian, coupling matrices have a storage capacity much larger than the Hebbian ones. Indeed the storage capacity  $C$  of random matrices scales exponentially with  $N$ :  $C \sim e^{\Sigma N}$  being  $\Sigma$  the complexity. The latter quantity is found to be maximised for asymmetric and diluted matrices, with values that match the connectivity found in the hippocampus areas.

The approach outlined in reference [1], as elaborated in the subsequent chapter, diverges from both the Hebbian and random connectivity models. It relies on a deterministic coupling matrix, which is derived from experimental observations of the connections between human brain regions. This approach assumes that the coupling strength is proportionally linked to a specific function of the distances between nodes (see Eq. 3):  $J_{ij} = e^{-d_{ij}/\delta}$ ,  $d_{ij}$  being the Euclidean distance between nodes  $i$  and  $j$  in the network. At variance with the latter approach, where the dynamics is based on the Hopf oscillator model, we here use the same coupling matrix of [1], but employ the Hopfield dynamics that, to the best of our knowledge, was never used to model whole brain activity dynamics.

Our main conclusions are summarized as follows:

*i)* We confirm the existence of a scaling regime of the neural activity in space for each value of the connectivity decay length  $\delta$  in the explored range,  $0 \leq \delta \leq 10$  mm.

*ii)* At  $\delta \sim 5.5$  mm we found  $\alpha \sim 2/5$ , very close to the one reported by Deco *et al.* [1] for the same value of  $\delta$ <sup>1</sup>.

*iii)* The scaling exponent shows a decreasing trend with the decay length  $\delta$ . Importantly, the functional relation  $\alpha(\delta)$  shows a steep increase in the region around  $\delta \sim 5.55$  mm, the value indicated in [1] as the physiologically relevant one. This means that the specific value of the decay length has a significant impact on the scaling exponent, for instance a slight increase to  $\delta = 6$  mm would yield a scaling exponent slightly above  $2/3$ , the value associated to homogenous incompressible turbulence. Conversely, a slight decrease to  $\delta = 5$  mm, would yield  $\alpha \sim 0.1$ , a much less organized regime. This pinpoints the importance of fine-tuning the value of  $\delta$ .

*iv)* By systematically pruning the couplings below a given running threshold,  $J_{ij} < J_{th}$  (which correspond to setting to zero the connection above a certain distance), it is found that the scaling exponent remains largely unaffected up to we get to pruning 95% - 98% of the couplings, suggesting that nodes at a distance  $d > \sim 5\delta$ , do not significantly partake to the physical mechanisms at the roots of the scaling regime. Accordingly, the model brain loses functionality by removing connections below  $6\delta$ , which is close to the geometric mean between the local scale  $\delta$  and the size of the global brain, about  $25\delta$ , circa 20 cm.

## THE TURBULENT-LIKE WHOLE-BRAIN MODEL

Deco *et al.* model the global human brain as a set of  $N$  coupled Hopf oscillators of the form

$$\frac{dx_i}{dt} = a_i x_i + (\beta y_i - x_i)(x_i^2 + y_i^2) - \omega_i y_i + G \sum_{j=1}^N J_{ij} (x_j - x_i) - \nu_i \xi_i \quad (1)$$

$$\frac{dy_i}{dt} = a_i y_i + (\beta x_i + y_i)(x_i^2 + y_i^2) - \omega_i x_i + G \sum_{j=1}^N J_{ij} (y_j - y_i) - \nu_i \xi_i \quad (2)$$

In the above,  $(x_i, y_i)$  are the real and imaginary part of the BOLD signal recorded at the  $i$ -th node of the network,  $a_i = -0.02$  are decay terms at the brink of the Hopf bifurcation, where scaling is best observed,  $\omega_i$  is the natural frequency of the oscillators,  $\beta$  the so called shear factor and  $\xi$  a gaussian noise with unit variance. The global coupling across the network is represented through the connectivity matrix  $J_{ij}$  which is assumed to obey the Exponential Distance Rule

$$J_{ij} = e^{-d_{ij}/\delta} \quad (3)$$

where  $d_{ij}$  is the euclidean distance between nodes  $i$  and  $j$  and we have set  $\delta$  ( $\equiv 1/\lambda$  in Deco's notation). [1] argues that the exponential distance rule matches very well the empirical HCP dMRI tractography of the human brain. In particular, it reproduces the decay of the fiber densities between the parcel centroid pairs as a function of the Euclidian distance. The authors [1] further show that the optimal fit is obtained for  $\delta = 5.55$  mm.

<sup>1</sup> In Ref. [1] the used parameter is the inverse of the decay scale,  $\lambda = 1/\delta$ .

### Amplitude of turbulence and scaling regime

In order to assess the scaling properties of the “turbulent brain” (TB), Deco *et al.* introduce the following complex Kuramoto Order Parameter:

$$\Psi_i(t) \doteq R_i(t)e^{i\theta_i(t)} \doteq \sum_{j=1}^N W_{ij}e^{i\phi_i(t)} \quad (4)$$

where  $W_{ij} = J_{ij} / \sum_{k=1}^N J_{ik}$  and  $\phi_i(t)$  is the phase of the  $i$ -th oscillator obtain by Hilbert-transform of the (narrow band) BOLD signal. The authors then measure the amplitude of turbulence as the variance of the fluctuations of amplitude of the order parameter, namely:

$$D \doteq \langle R^2 \rangle - \langle R \rangle^2 \quad (5)$$

where bracket indicate average in space and time over the entire network and over hundreds of noise realizations.

The scaling regime is assessed by inspecting the associated structure function

$$S_2(d) = \langle (R(x+d) - R(x))^2 \rangle \sim d^\alpha \quad (6)$$

where “ $x$ ” and “ $x+d$ ” indicate that the two network nodes are at distance  $d$  and the average is taken at statistical steady state, over all network nodes and noise realizations. This observable is commonly used to assess the statistical properties of fluid turbulence, and for the case of Kolmogorov homogeneous incompressible turbulence one obtains

$$\alpha_T = 2/3,$$

indicating that the change in the (longitudinal) flow field at a distance  $d$ ,  $\delta u(d) = \langle |u(x+d) - u(x)| \rangle$ , scales like  $d^{1/3}$ , hence the turbulent flow field is not differentiable (sometimes  $\alpha$  is also called the roughness exponent) [27, 28]. For the whole-brain model, Deco *et al.* [1] report

$$\alpha_D \sim 1/2,$$

indicating that the correlation pattern of the brain signals is *less* regular than those observed in homogeneous incompressible turbulence.

As we shall show, these values should be taken with extreme caution, as they are very sensitive to a number of assumptions, primarily the structure and functional dependence of the connectivity matrix on the internode distance.

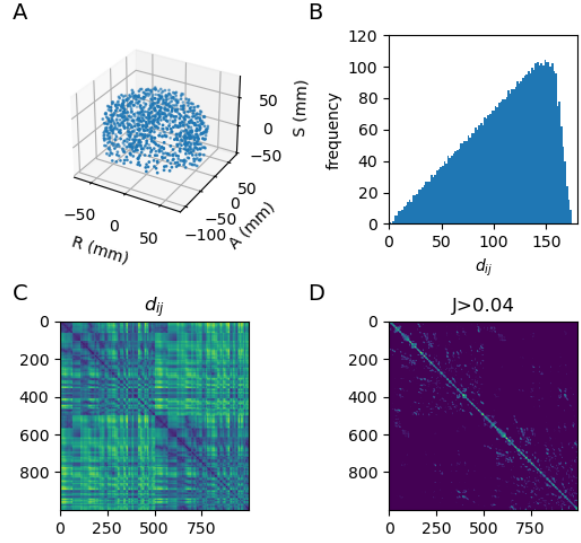


FIG. 1. A) 1000 parcel centroids in three dimensional space from Schaefer’s cerebral cortical parcellation atlas [29]. B) Frequency histogram of the Euclidean distances  $d_{ij}$  between each pair of nodes from Schaefer’s cerebral cortical parcellation atlas [29]. The linear dependence on  $d_{ij}$  indicates that the nodes are basically distributed on a two dimensional surface. C) Matrix composed of the Euclidean distances  $d_{ij}$  between each pair of nodes from Schaefer’s cerebral cortical parcellation atlas [29]. D) Matrix formed by the values such that  $J_{ij} > 0.4$ , where  $J_{ij} = e^{-d_{ij}/\delta}$  with  $\delta=0.55$ .

### DISCRETE-TIME HOPFIELD RECURRENT NEURAL NETWORKS

Following [2–5, 12, 19, 24, 30], we consider a network of  $N$ -binary neurons that can be either firing or silent.

The state of each neuron is a binary variable  $s_i$ , with  $i = 1, 2, \dots, N$ , such that  $s_i = -1$  or  $s_i = 1$ , so that the network state is represented by a binary string  $\mathbf{s} = (s_0, s_1, \dots, s_N)$ . Neurons interact through the connectivity matrix  $\mathbf{J}$ , with matrix elements  $J_{ij}$  following the same exponential dependence  $J_{ij} = e^{-d_{ij}/\delta}$  used in [1]. We assume a discrete time  $t$ , and, at each time step  $t$ , the evolution of the neuron state  $s_i(t)$  is given by the following non-linear dynamic equation,

$$s_i(t+1) = \text{sign} \left[ \sum_{j=1}^N J_{ij} s_j(t) \right], \quad (7)$$

where the activation function  $\text{sign}(x)$  is defined such as  $\text{sign}(x) = 1$  for  $x \geq 0$ , and  $\text{sign}(x) = -1$  otherwise. Consequently, whenever the summation

of the inputs on neuron  $i$  is above zero, the neuron is active (“fires”), otherwise, it remains silent.

### The structural connectivity

We determined the Hopfield Brain connectivity using Schaefer’s cerebral cortical parcellation atlas. This parcellation was obtained from the analysis of a large dataset with a sample size of 1489 [29]. This dataset is publicly available, we used Schaefer’s 1000 parcellation with parcel centroids mapped onto the MNI152 volumetric space<sup>2</sup>. Fig. 1A shows the spatial distribution of the centroids in the MNI152 volumetric space. From the centroids of these areas, we computed the pairwise distances. Fig. 1B shows the histogram of the pair distances  $d_{ij}$  between each couple of centroids. Figures 1C and D show respectively the matrix composed of the Euclidean distances  $d_{ij}$ , the matrix obtained with the threshold  $J_{ij} > 0.4$  were  $J_{ij} = e^{-d_{ij}/\delta}$  with  $\delta=0.55$ .

### THE STRUCTURE FACTOR $S_2(d)$

We used [1] adaptation of Kolmogorov’s concept of structure functions. In turbulence, the Kolmogorov’s structure factor applies to the longitudinal velocity but in our case it represents the activity of the parcel which as measured through the BOLD signal in a fMRI experiment.

To compute the structure factor we use the auxiliary function  $B(d)$  defined as:

$$B(d) = \frac{1}{T} \sum_{t=1}^T \frac{1}{\mathcal{N}(d)} \sum_{d_{ij} \in d} s_i(t) s_j(t) \quad (8)$$

where the function  $\mathcal{N}(d)$  represents the number of  $i, j$  pairs at distance  $d$ . The notation  $d_{ij} \in d$  indicates that the distance between the nodes must be “close enough” to  $d$ . To this aim, it should be kept in mind that in Schaefer’s cerebral cortical parcellation atlas,  $d$  was recorded with 2mm precision, thus there are multiple  $i, j$  pairs with the same  $d$ . Therefore we can bin the existing nodes’ distance and map them to the natural numbers, so as to use of the Kronecker delta  $\Delta(ij|d)$ , which takes value 1 if  $d_{ij}$  is in the bin identified by  $d$ , and is 0 otherwise.

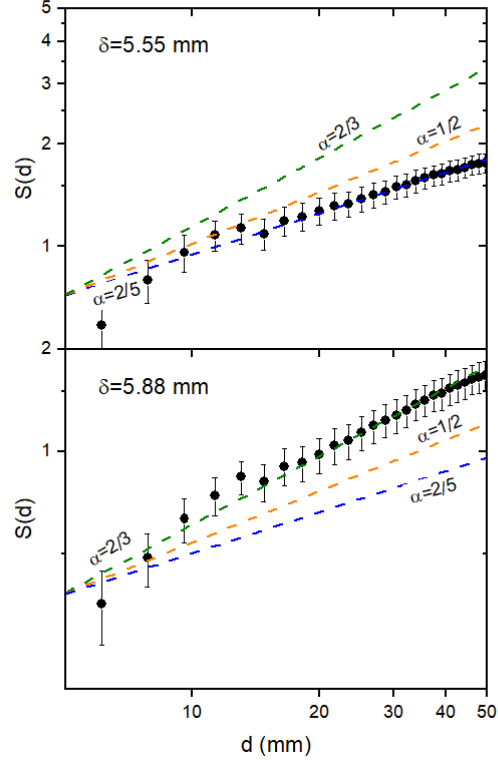


FIG. 2. Structure factor  $S_2(d)$  for  $N_r = 40$  realizations respectively at  $\delta = 5.55$  mm (A), and  $\delta = 5.88$  mm (B). The values  $S_2(d)$  were binned over equal sized intervals. The dashed lines indicate different  $\alpha$  values:  $\alpha = 2/3$  which corresponds to turbulence,  $\alpha = 1/2$ , the value obtained in [1], and  $\alpha = 2/5$ . We estimate the scaling exponent  $\alpha$  with a linear regression of  $\log(S(d)) \sim \alpha \log(d) + \beta$  in the interval range  $[2.7 - 33.1]$  mm, as used in [1], and we obtain  $\alpha \approx 2/5$  for  $\delta = 5.55$  mm, and  $\alpha \approx 2/3$  for  $\delta = 5.88$  mm.

As a result, we have:

$$B(d) = \frac{1}{T} \sum_{t=1}^T \frac{1}{\mathcal{N}(d)} \sum_{ij} s_i(t) s_j(t) \Delta(ij|d) \quad (9)$$

and

$$\mathcal{N}(d) = \sum_{ij} \Delta(ij|d) \quad (10)$$

The function  $B(d)$  relates to the structure factor as follows:

$$\begin{aligned} S_2(d) &\doteq \frac{1}{T} \sum_{t=1}^T \frac{1}{\mathcal{N}(d)} \sum_{ij} (s_i(t) - \bar{s})(s_j(t) - \bar{s}) \Delta(ij|d) \\ &= 2[B(0) - B(d)] \end{aligned} \quad (11)$$

<sup>2</sup> Github repository dataset url [29]: [https://github.com/ThomasYeoLab/CBIG/tree/master/stable\\_projects/brain\\_parcellation/Schaefer2018\\_LocalGlobal/Parcellations/MNI/Centroid\\_coordinates](https://github.com/ThomasYeoLab/CBIG/tree/master/stable_projects/brain_parcellation/Schaefer2018_LocalGlobal/Parcellations/MNI/Centroid_coordinates)

The Hopfield dynamics is deterministic, and since the phase space of the nodes' states is finite, the asymptotic trajectories must necessarily be periodic. Therefore, as also discussed in [30], Hopfield Recurrent Neural Networks, given an initial state, consistently ends up into a specific steady state ("attractor"). The steady states are deterministic attractors composed of either limit cycles formed by repeating sequence of states, or a single stationary state. Under the parametrizations considered here, we numerically found that the steady states were always composed of a single fixed point, as expected in the case of symmetric couplings  $J_{ij}$ . In the absence of a further external input ("external stimuli"), the network (the brain) is stuck in the attractor and the whole activity is constant in time, hence no time summation was taken in the previous equations. This is of course a very crude representation of the brain dynamics, which receives continuously "internal" and "external" inputs, but we can think at the whole set of attractors as a reasonable representation of the dynamical correlations within the whole brain model.

Given different values of the decay length  $\delta$ , we have run the Hopfield model for a system composed by  $N = 1000$  neurons (with pairwise distances consistent with the Schaefer's cerebral cortical parcellation atlas [29]). The structure functions have then been calculated by following the system until the fixed points were reached, and by averaging over  $N_r = 40$  randomly chosen initial states. Figure 2 shows the structure factor  $S_2(d)$  for respectively  $\delta = 5.55$  mm (Fig. 2A) and  $\delta = 5.88$  mm (Fig. 2B). The black points with the error bars represent the average  $S(d)$  computed over 40 different realizations. The dashed green line corresponds to  $\alpha = 2/3$ , the orange line corresponds to  $\alpha = 1/2$ , and the blue line corresponds to  $\alpha = 2/5$ . The  $\alpha = 1/2$  value (green line) is the value estimated in [1]. The  $\alpha = 2/3$  is the exponent associated with a turbulence. Due to the significant level of statistical fluctuations, we have estimated the average exponent in two different ways, first as the correct ensemble average  $\langle S_2(d) \rangle \sim d^\alpha$  and also as an arithmetic average of the single realization exponents,  $\bar{\alpha} = N_r^{-1} \sum_{r=1}^{N_r} \alpha_r$ . Even though the latter is not correct, the fact that both yield very similar values attests to the robustness of the average exponent, notwithstanding sizeable fluctuations. We estimate the scaling exponent  $\alpha$  in the interval  $[2.7 - 33.1]$  mm as in [1] and we obtained  $\alpha \approx 2/5$  for  $\delta = 5.55$  mm, and  $\alpha \approx 2/3$  for  $\delta = 5.88$  mm.

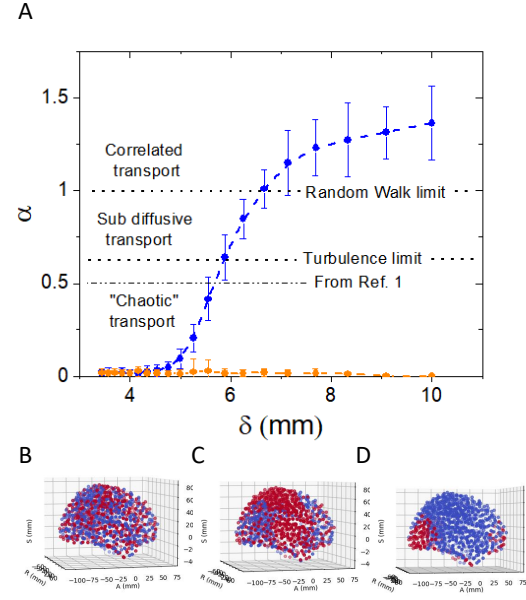


FIG. 3. A) The blue line shows the average slope of  $\alpha = \log S(d) / \log d$  for different  $\delta$ s, given the connectivity matrix  $J_{ij} = \exp(-d_{i,j}/\delta)$ . The horizontal dotted lines correspond to  $\alpha_{RW} = 1$  and  $\alpha_T = 2/3$ , corresponding to random walk and homogeneous incompressible turbulence, respectively, while the dot-dashed horizontal line corresponds to Deco *et al.* "brain" value  $\alpha_D = 1/2$ . The orange line shows the function  $\alpha(\delta)$  with a connectivity matrix obtained by randomly shuffling all the weights  $J_{ij}$ , which results into a basically uncorrelated signal, indicating the importance of the metric structure of the weights. The plot stops at  $\delta = 10$ , a region where the signal is highly correlated ( $\alpha \sim 1.4$ ), but still below the smooth regime marked by  $\alpha = 2$ . A visual extrapolation indicates that the scaling regime would remain non-smooth ( $\alpha < 2$ ) even in the limit of an "infinite-brain",  $\delta \rightarrow \infty$ , the global brain ( $d \sim 25\delta$ ) being pretty close to the infinite-brain limit. Note however that in this region  $B(d) \sim B(0)$ , so that the numerical calculation of the exponent becomes less and less accurate (a fully correlated signal with  $B(d) = B(0)$  yields formally  $\alpha \rightarrow \infty$ ). Conversely, a brain below 4 mm, would exhibit "chaotic" behaviour, with scaling exponents close to zero, i.e. no scaling regime. The bottom panel shows the neuron activity mapped on the Schaefer's cerebral cortical parcellation atlas coordinates for (B)  $\delta = 4$  ("chaotic"), (C)  $\delta = 5.99$ , and (D)  $\delta = 6.66$  (random walk), respectively.

#### Scaling exponents as a function of the decay length

We repeated the previously depicted procedure for a sequence of values of the decay length in the range  $[3 - 10]$  mm and measured the associated scaling exponents. The values of  $\alpha(d)$  for different realizations

are shown in Fig.3.

Several comments are in order. First, we observe a clear increasing trend of  $\alpha$  with  $\delta$ , meaning that small decay lengths, *i.e.* localised connectivity, promotes irregular patterns. For instance, below  $\delta \sim 4$  mm, the scaling exponent is basically zero, corresponding to complete randomness. This was checked independently, by running simulations in which the couplings  $J_{ij}$  were randomized though keeping the same distribution of the elements of the matrix  $J$  (flat orange line at the bottom). We were able to simultaneously randomize the couplings  $J_{ij}$ , and keep the same value distribution by randomly shuffling the  $J_{ij}$  values. At the opposite end, with  $\delta = 10$  mm, we measure  $\alpha \sim 1.4$ , which is still well below the smoothness threshold  $\alpha_S = 2$ , but above the random walk value  $\alpha_R = 1$ , and much above the Kolmogorov turbulence value  $\alpha_T = 2/3$ , which is in turn larger than  $\alpha_D \sim 1/2$ , the value obtained by Deco *et al.* at  $\delta \sim 5.55$  mm. Importantly, in the intermediate regime, around the physiological value  $\delta = 5.55$  mm, the present Hopfield model delivers  $\alpha_H \sim 2/5$ , different but still close to Deco *et al.* value.

Figure 4 shows how the pair correlation for different values of  $\delta$ . For  $\delta < 5$  mm, the pair correlation shows a basically uncorrelated activity, except at short range. For  $\delta = 5.26$  mm, long-range pair correlations start to emerge and finally, for larger  $\delta$ , the long-range pair correlations become even stronger. In the limit of very large  $\delta$ , stationary states emerge in which the system freezes into a single fully-ordered state, with all nodes states either +1 or -1.

Our analysis confirms that there is indeed a scaling regime in the organization of the brain patterns which reminds fluid turbulence, yet with a higher degree of spikiness. Indeed, by sticking to the physiological value  $\delta = 5.55$  mm, the Hopfield brain appears more irregular (lower scaling exponent) than a random walk and also of homogeneous incompressible turbulence. The most important feature, though, is the sigmoidal dependence of the relation  $\alpha = \alpha(\delta)$  with the rampup region between about 4 and 7 mm, centered around  $\delta \sim 5.9$ . This is indeed a physiologically relevant scale of local regions in the brain. Furthermore, this rampup region unveils the major sensitivity of the scaling exponent to small changes of the decay length, indicating that small changes of the decay length lead to fairly different scaling regimes. In particular, for  $\delta$  below 4 mm, the activity appears to be nearly chaotic, whereas for  $\delta$  above 8 mm, it becomes kind of “rigid”, *i.e.* globally correlated.

A word of caution must be spent on the statisti-

cal accuracy of the scaling exponents, which for the present case of 40 realizations, is around 25 percent.

## THRESHOLDING THE CONNECTIONS

Having assessed that delocalization (large  $\delta$ s) promotes a correlated response, it is natural to inquire the role of short versus long-range couplings in promoting the correlated patterns sustaining the scaling regime.

To this purpose, we performed a series of simulations by progressively removing pairs of nodes whose coupling strengths lie below a given threshold, namely  $J_{ij} < J_{th}$ , where the coupling strengths vary in the range [0, 1]. Since  $J_{ij}$  decays exponentially with the pair distance, it is clear that the running threshold removes first the distant nodes and then the less distant ones, upon increasing the threshold, thereby implementing a “correlated dilution” process. More precisely, a threshold  $J_{th}$  excludes pairs beyond a distance

$$d_{th} = \delta \ln(1/J_{th}), \quad (12)$$

thereby retaining only a fraction  $1 - J_{th}$  of the full set of interacting nodes. The result of this progressive dilution on the scaling exponent are reported in Figure 5. Where the dilution  $\rho$  is defined as the fraction of disconnected nodes  $i, j$ ,  $J_{ij} = 0$ , and the result on the scaling exponent is measured comparing the undiluted exponent  $\alpha(0)$  with the exponent  $\alpha(\rho)$  at that dilution. Since the dilution is obtained thresholding in order the  $J_{ij}$  values until we get a certain fraction of disconnected nodes, and since eq. 12 we get that to a certain dilution corresponds a certain cutoff distance above which all couples are disconnected.

From this figure, a smooth trend at increasing  $\rho$  is observed, with the scaling exponent starting to display significant decrease above  $\rho = [0.95, 0.98]$ , when just 2 or 5 percent of the nodes are left, corresponding to  $d_{ij} > 4.6\delta$ . With  $J_{th} = 0.10$ , corresponding to  $d_{ij} > -\delta \ln(0.1) \sim 0.46\delta$ , the scaling exponent is basically halved, indicating a major loss of correlation. This is expected since  $J_{th} = 0.10$  cuts out all but shortest range interactions.

The conclusion of this dilution analysis is that the brain response is carried almost entirely by interactions up to about five decay lengths, namely about 1/5 of the size of the global brain. This sounds reasonable, as it strikes a plausible compromise between short-range ( $d < 4\delta$ ) and long-range ( $d > 6\delta$ ) interactions. It is interesting to observe that a “solid”

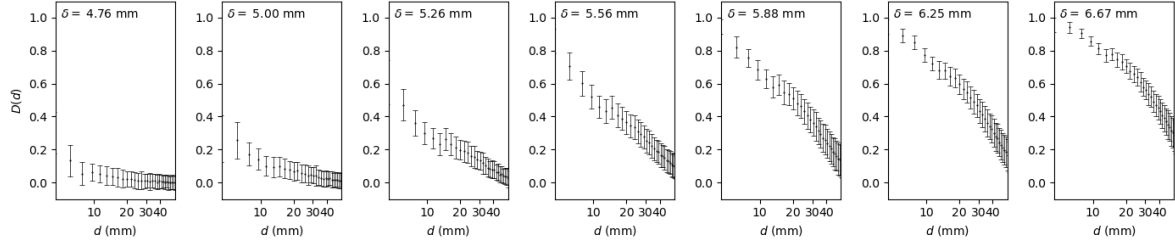


FIG. 4. Pair-correlation functions  $B(d)$  for different  $\delta$ s. At small  $\delta$  the signal is largely uncorrelated, while at increasing  $\delta$ , correlations start to emerge, although affected by significant amount of statistical fluctuations.

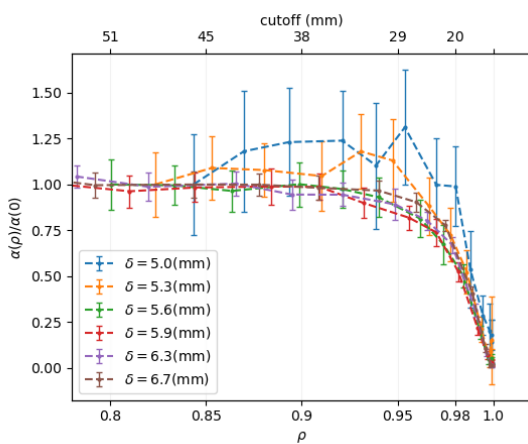


FIG. 5. The average slope of  $\log S(d)$  for different dilution levels  $\alpha(\rho)$ , normalized to its threshold-free value  $\alpha(0)$  at that given  $\delta$ . The dilution is measured as the fraction of disconnected pairs  $i, j$ ,  $J_{ij}$  elements with value 0. The second  $y$ -axis on top shows the cutoff distance in mm for which at a certain dilution  $\rho$  the pairs at a larger or euql distance are disconnected. The differently colored curves indicate simulations with different  $\delta$  values. The graph shows that within the measurement error, the system is not affected by the dilution of the edges, up to the removal of more than the 95% of the connections, in descending order of distance. This shows that, in view of the exponential connectivity  $J_{ij} = e^{-d_{ij}/\delta}$ , the onset of collective patterns is sustained mostly by the close connections, within about 4 $\delta$ .

(strongly correlated) brain, such as the one that results for  $\delta > 10$  mm, would be too homogeneous to be able to store and process the amount of information required to function properly.

On the opposite side, for too short connectivity length, the brain would behave like a “gas” of disconnected neurons, hence incapable of collective behavior, which is key to its proper functioning.

It appears like the physiological length is achieving an optimal compromise between these two opposite,

order-disorder, trends. With a daring but conducive metaphor, we could speculate that the brain works in a sort of turbulent liquid-like state, although more spiky than actual turbulent fluids.

## CONCLUSIONS

It is shown that an Hopfield recurrent neural network, informed by experimentally derived brain topology, recovers the scaling picture recently proposed by Deco [1], according to which the process of information exchange within the human brain shows spatially correlated patterns qualitatively similar to those displayed by turbulent flows.

Our analysis confirms the initial finding by [1] in near-quantitative form, predicting very similar scaling exponent for the same value of the connectivity decay length. This is pretty remarkable, given the very different nature of the two mathematical models and provides a strong hint at the robustness of the scaling picture.

It is further observed that the scaling exponents are smaller than for the case of turbulence, indicating that the collective activity of the brain is more irregular (spiky) than for a homogeneous incompressible turbulent fluid.

Importantly, the scaling exponents show a steep dependence on the spatial range of neural connections, hence the specific value of the decay length has a major impact on the degree of irregularity (spikiness) of the collective patterns.

This provides a strong indication that there is an optimal connectivity length at which the brain shows non-smooth functional behavior. This appears to happen at a scale around 5,5 mm, hence well below the global size of the brain. Longer/shorter connectivities would lead to excessive smoothness/roughness respectively. Interestingly, a dilution analysis shows that the Hopfield model brain remains functional by removing links

above about six decay lengths, namely 25 – 30 mm, corresponding to about one fifth of the size of the global brain. This indicates that, in terms of connectivity decay length, the brain seems to function in a sort of intermediate "turbulent liquid-like" state , whose essential connections lie in near geometrical mean between the decay length and the global size of the brain. This turbulent liquid-like state appears to be more spiky than ordinary homogeneous incompressible turbulent fluids.

## ACKNOWLEDGMENTS

One of the authors (SS) wishes to acknowledge financial support from the Bertarelli Foundation during his stay at the Neurobiology Department of the Harvard Medical School. The authors wish to acknowledge illuminating discussions with John A. Assad, Haim Sompolinsky, and Bernardo Sabattini. GG contributes to code writing and simulations. GG, SS, and GR conceived the Idea, designed the experiments, interpreted the data, and wrote the manuscript.

## BIBLIOGRAPHY

---

- [1] G. Deco and M. L. Kringelbach, "Turbulent-like dynamics in the human brain," *Cell Reports*, vol. 33, p. 108471, 12 2020.
- [2] S. I. Amari, "Learning patterns and pattern sequences by self-organizing nets of threshold elements," *IEEE Transactions on Computers*, vol. C-21, pp. 1197–1206, 1972.
- [3] W. A. Little, "The existence of persistent states in the brain," *Mathematical Biosciences*, vol. 19, pp. 101–120, 2 1974.
- [4] J. J. Hopfield, "Neural networks and physical systems with emergent collective computational abilities," *Proceedings of the National Academy of Sciences of the United States of America*, vol. 79, pp. 2554–2558, apr 1982.
- [5] D. J. Amit, H. Gutfreund, and H. Sompolinsky, "Storing Infinite Numbers of Patterns in a Spin-Glass Model of Neural Networks," *Physical Review Letters*, vol. 55, pp. 1530–1533, sep 1985.
- [6] N. Brunel, "Is cortical connectivity optimized for storing information?," *Nature Neuroscience*, vol. 19, pp. 749–755, may 2016.
- [7] C. J. Hillar and N. M. Tran, "Robust Exponential Memory in Hopfield Networks," *Journal of Mathematical Neuroscience*, vol. 8, no. 1, 2018.
- [8] C. Hillar, T. Chan, R. Taubman, and D. Rolnick, "Hidden Hypergraphs, Error-Correcting Codes, and Critical Learning in Hopfield Networks," *Entropy* 2021, Vol. 23, Page 1494, vol. 23, p. 1494, nov 2021.
- [9] D. Stauffer, A. Aharony, L. D. F. Costa, and J. Adler, "Efficient hopfield pattern recognition on a scale-free neural network," *The European Physical Journal B - Condensed Matter and Complex Systems* 2003 32:3, vol. 32, pp. 395–399, 2003.
- [10] D.-H. Kim, J. Park, and B. Kahng, "Enhanced storage capacity with errors in scale-free hopfield neural networks: An analytical study," *PLOS ONE*, vol. 12, p. e0184683, 10 2017.
- [11] V. Folli, G. Gosti, M. Leonetti, and G. Ruocco, "Effect of dilution in asymmetric recurrent neural networks," *Neural Networks*, vol. 104, pp. 50–59, 8 2018.
- [12] M. Leonetti, V. Folli, E. Milanetti, G. Ruocco, and G. Gosti, "Network dilution and asymmetry in an efficient brain," *Philosophical Magazine*, vol. 100, pp. 2544–2555, oct 2020.
- [13] K. Gopalsamy and X. zhong He, "Stability in asymmetric hopfield nets with transmission delays," *Physica D: Nonlinear Phenomena*, vol. 76, pp. 344–358, 9 1994.
- [14] Z.-B. Xu, G.-Q. Hu, and C.-P. Kwong, "Asymmetric hopfield-type networks: Theory and applications," *Neural Networks*, vol. 9, pp. 483–501, 4 1996.
- [15] T. Chen and S. I. Amari, "Stability of asymmetric hopfield networks," *IEEE Transactions on Neural Networks*, vol. 12, pp. 159–163, 1 2001.
- [16] F. M. Franca and Z. Yang, "Building artificial cpns with asymmetric hopfield networks," *Proceedings of the International Joint Conference on Neural Networks*, vol. 4, pp. 290–295, 2000.
- [17] P. Zheng, J. Zhang, and W. Tang, "Analysis and design of asymmetric hopfield networks with discrete-time dynamics," *Biological Cybernetics*, vol. 103, pp. 79–85, 7 2010.
- [18] A. Szedlak, G. Paternostro, and C. Piermarocchi, "Control of asymmetric hopfield networks and application to cancer attractors," *PLOS ONE*, vol. 9, p. e105842, 8 2014.
- [19] G. Gosti, E. Milanetti, V. Folli, F. de Pasquale, M. Leonetti, M. Corbetta, G. Ruocco, and S. Della Penna, "A recurrent hopfield network for estimating meso-scale effective connectivity in meg," *Neural Networks*, vol. 170, pp. 72–93, 2024.
- [20] D. O. Hebb, *The Organization of Behavior; A Neuropsychological Theory*. Wiley, 10 1949.
- [21] A. Fachechi, E. Agliari, and A. Barra, "Dreaming neural networks: Forgetting spurious memories and reinforcing pure ones," *Neural Networks*, vol. 112, 2019.
- [22] M. Benedetti, E. Ventura, E. Marinari, G. Ruocco, and F. Zamponi, "Supervised perceptron learning vs unsupervised hebbian unlearning: Approaching optimal memory retrieval in hopfield-like networks," *Journal of Chemical Physics*, vol. 156, 2022.
- [23] M. Benedetti and E. Ventura, "Training neural networks with structured noise improves classification

and generalization,” *arXiv*, vol. 2302.13417v4, 2 2023.

[24] G. Gosti, V. Folli, M. Leonetti, and G. Ruocco, “Beyond the Maximum Storage Capacity Limit in Hopfield Recurrent Neural Networks,” *Entropy*, vol. 21, p. 726, jul 2019.

[25] S. Hwang, V. Folli, E. Lanza, G. Parisi, G. Ruocco, and F. Zamponi, “On the number of limit cycles in asymmetric neural networks,” *Journal of Statistical Mechanics: Theory and Experiment*, vol. 2019, p. 053402, 5 2019.

[26] S. Hwang, E. Lanza, G. Parisi, J. Rocchi, G. Ruocco, and F. Zamponi, “On the number of limit cycles in diluted neural networks,” *Journal of Statistical Physics*, vol. 181, pp. 2304–2321, 12 2020.

[27] U. Frisch, *Turbulence*. Cambridge University Press, 11 1995.

[28] R. Benzi, S. Ciliberto, R. Tripiccione, C. Baudet, F. Massaioli, and S. Succi, “Extended self-similarity in turbulent flows,” *Physical Review E*, vol. 48, p. R29, 7 1993.

[29] A. Schaefer, R. Kong, E. M. Gordon, T. O. Lau-  
mann, X.-N. Zuo, A. J. Holmes, S. B. Eickhoff, and  
B. T. T. Yeo, “Local-global parcellation of the hu-  
man cerebral cortex from intrinsic functional con-  
nectivity mri,” *Cerebral Cortex*, vol. 28, pp. 3095–  
3114, 9 2018.

[30] V. Folli, M. Leonetti, and G. Ruocco, “On the Max-  
imum Storage Capacity of the Hopfield Model,”  
*Frontiers in Computational Neuroscience*, vol. 10,  
p. 144, jan 2017.